

Antisymmetric \mathcal{PT} -photonic structures with balanced positive and negative index materials

Li Ge* and H. E. Türeci

Department of Electrical Engineering, Princeton University, Princeton, New Jersey 08544

In this Letter we study a new class of synthetic materials in which the refractive index satisfies a special symmetry, $n(-\mathbf{x}) = -n^*(\mathbf{x})$, which we term antisymmetric parity-time (\mathcal{APT}) systems. Unlike \mathcal{PT} -symmetric systems which require balanced gain and loss, i.e. $n(-\mathbf{x}) = n^*(\mathbf{x})$, \mathcal{APT} systems consist of balanced positive and negative index materials (NIMs). Despite the seemingly \mathcal{PT} -symmetric optical potential $V(\mathbf{x}) \equiv n(\mathbf{x})^2\omega^2/c^2$, such systems are not invariant under combined \mathcal{PT} operation due to the discontinuity of the spatial derivative of the wavefunction. We show that \mathcal{APT} systems display intriguing properties such as spontaneous phase transition of the scattering matrix, bidirectional invisibility, and a continuous lasing spectrum.

PACS numbers: 41.20.Jb, 42.25.Bs, 42.55.Ah

Parity-time (\mathcal{PT}) symmetric systems have attracted considerable interests since the original work by Bender and colleagues [1–3], both in the fields of quantum mechanics and photonics. In \mathcal{PT} -symmetric quantum mechanics the Schrödinger equation does not have time-reversal symmetry but is invariant under combined parity-time operation. The corresponding Hamiltonian is non-Hermitian, yet it displays regions of real energy spectrum and was speculated as an alternative to canonical quantum mechanics. The idea was introduced into photonics by Christodoulides and coworkers [4, 5], utilizing balanced gain and loss ($n(-\mathbf{x}) = n^*(\mathbf{x})$) to satisfy the \mathcal{PT} -symmetry. Many intriguing optical phenomena have since been predicted and observed, such as double refraction [5], power oscillations [5–7], coexistence of coherent perfect absorption [8, 9] and lasing states [10, 11], spontaneous symmetry breaking of the scattering matrix [11], and unidirectional transmission resonances [12, 13].

Another field that has attracted tremendous research interests is negative index materials (NIM) [14–17]. In such materials the refractive index is negative over some frequency range, achieved by using engineered resonances of nanostructures in metamaterials. NIMs have been proposed to realize subwavelength imaging (i.e. “superlense” [14]) and dramatically change light-matter interaction via altered local density of optical states [18]. NIMs are strongly absorptive, but recent advances with imbedded active media have demonstrated reduced intrinsic loss and even net gain [19].

In this Letter we study a class of new systems bridging NIMs and \mathcal{PT} -symmetric photonics. Their refractive index is *antisymmetric* under combined \mathcal{PT} operation, $n(-\mathbf{x}) = -n^*(\mathbf{x})$, i.e. with balanced positive index materials (PIMs) and NIMs; the imaginary part of $n(\mathbf{x})$ is symmetric, which can be positive (loss), negative (gain), zero, or any complicated spatial function. Outside the system we assume that the refractive index is uniform, symmetric, and positive. We term such synthetic sys-

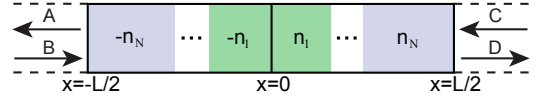


FIG. 1. (Color online) Schematic of a 1D \mathcal{APT} photonic heterostructure, consisting of $2N$ layers that satisfy $n(x) = -n(-x)^*$.

tems antisymmetric parity-time (\mathcal{APT}) systems, which display intriguing features such as bidirectional invisibility, spontaneous phase transition of the S-matrix, and a continuous lasing spectrum.

We base our discussion on the scalar wave equation for the electric field

$$[\nabla^2 + n(\mathbf{x})^2 (\omega^2/c^2)] E(\mathbf{x}; \omega) = 0, \quad (1)$$

which describes steady-state solutions in one-dimensional (1D) and two-dimensional (2D) systems. Henceforth we set $c = 1$ and assume that the corresponding $\mu_{\text{NIM}} = -|\mu_{\text{PIM}}|$ if $n_{\text{NIM}} = -n_{\text{PIM}}^*$. By first glance one may misjudge that all the intriguing phenomena found in conventional \mathcal{PT} -symmetric systems would survive since the optical potential $V(\mathbf{x}) \equiv n(\mathbf{x})^2\omega^2$ is still invariant under \mathcal{PT} operation. We note that this is not true since the boundary condition at PIM and NIM interfaces is now different. Take a 1D \mathcal{APT} heterostructures for example (see Fig. 1), the electric field itself is still continuous at PIM and NIM interfaces, but its spatial derivation now satisfies [20, 21]

$$\frac{1}{\mu_{\text{PIM}}} \frac{\partial E(x; \omega)}{\partial x} \Big|_{x \in \text{PIM}} = \frac{1}{\mu_{\text{NIM}}} \frac{\partial E(x; \omega)}{\partial x} \Big|_{x \in \text{NIM}}, \quad (2)$$

which changes abruptly due to the sign difference of μ_{PIM} and μ_{NIM} . Below We first analyze wave propagation and lasing in such 1D \mathcal{APT} heterostructures, followed by a discussion of pseudo- \mathcal{APT} symmetry for wave propagation in 2D with the paraxial approximation.

In Ref. [11] the phase transition of the scattering matrix (S-matrix) in a \mathcal{PT} -symmetric system is predicted based on the invariance of the system under combined

* lge@princeton.edu

\mathcal{PT} operations; We would not expect a similar phase transition in \mathcal{APT} systems, since flipping the sign of the real part of the refractive index is not related to any symmetry operation of the physical state. However, there do exist some special properties of the transmission coefficient t and the left and right reflection coefficients r_L, r_R in a 1D \mathcal{APT} heterostructure:

$$r_L = r_R^*, \quad \text{Im}[t] = 0. \quad (3)$$

To understand these properties, we start by noting one observation: By changing the refractive index of each layer in an *arbitrary* photonic heterostructure to its negative complex conjugate and flipping the sign the magnetic permeability, i.e. $n_i \rightarrow -n_i^*, \mu_i \rightarrow -\mu_i$, the transfer matrix M [22], defined by

$$\begin{pmatrix} A \\ B \end{pmatrix} = M \begin{pmatrix} C \\ D \end{pmatrix}, \quad (4)$$

becomes its complex conjugate at the same *real* frequency:

$$M(\omega) \rightarrow M^*(\omega), \quad \text{Im}[\omega] = 0. \quad (5)$$

The field amplitudes A, B, C , and D are defined in Fig. 1, or more specifically,

$$E(x; \omega) = \begin{cases} Ae^{-in_0\omega(x+L/2)} + Be^{in_0\omega(x+L/2)}, & x < -L/2, \\ Ce^{-in_0\omega(x-L/2)} + De^{in_0\omega(x-L/2)}, & x > L/2, \end{cases} \quad (6)$$

where n_0 is the refractive index outside the heterostructure and we have assumed $\mu_0 = 1$. The proof of (5) is straightforward from the analytical expression of M :

$$M(\omega) = D_0^{-1} [\Pi_{i=1}^N m_i] D_0, \quad (7)$$

obtained from the continuity of $E(x; \omega)$ and Eq. (2). The matrices D_0 and m_i are given by

$$D_0 = \begin{pmatrix} 1 & 1 \\ n_0 & -n_0 \end{pmatrix}, \quad (8)$$

$$m_i(\omega) = \begin{pmatrix} \cos(n_i\omega\Delta_i) & i\frac{\mu_i}{n_i} \sin(n_i\omega\Delta_i) \\ i\frac{n_i}{\mu_i} \sin(n_i\omega\Delta_i) & \cos(n_i\omega\Delta_i) \end{pmatrix}, \quad (9)$$

where Δ_i is the width of the i th layer. Under the transformation $n_i \rightarrow -n_i^*, \mu_i \rightarrow -\mu_i$ ($i = 1, \dots, N$), one finds $m_i(\omega) \rightarrow m_i^*(\omega)$ at a *real* frequency and so does $M(\omega)$. Since $M(\omega)$ determines the wave propagation, all related quantities, such as r_L, r_R, t or equivalently the S-matrix, become their complex conjugate under this transformation.

We refer to the left half of an \mathcal{APT} system U and the right half V . Eq. (5) implies that the transfer matrices of U and V are related by

$$M_V(\omega) = \sigma[M_U^{-1}(\omega)]^* \sigma, \quad \sigma = \begin{pmatrix} 0 & 1 \\ 1 & 0 \end{pmatrix}. \quad (10)$$

If we define $M_U(\omega) \equiv \begin{pmatrix} m_{11} & m_{12} \\ m_{21} & m_{22} \end{pmatrix}$ and the transfer matrix of the whole \mathcal{APT} system $M_{\mathcal{APT}}(\omega) \equiv \begin{pmatrix} m'_{11} & m'_{12} \\ m'_{21} & m'_{22} \end{pmatrix}$, we then find through $M_{\mathcal{APT}}(\omega) = M_U(\omega)M_V(\omega)$ that

$$\begin{aligned} m'_{11} &= |m_{11}|^2 - |m_{12}|^2, \\ m'_{22} &= |m_{22}|^2 - |m_{21}|^2, \\ m'_{12} &= m_{12}m_{22}^* - m_{11}m_{21}^* = -(m'_{21})^*. \end{aligned} \quad (11)$$

The S-matrix defined by

$$\begin{pmatrix} A \\ D \end{pmatrix} = S_{\mathcal{APT}} \begin{pmatrix} B \\ C \end{pmatrix} \equiv \begin{pmatrix} r_L & t \\ t & r_R \end{pmatrix} \begin{pmatrix} B \\ C \end{pmatrix} \quad (12)$$

can be easily expressed in terms of $M_{\mathcal{APT}}$:

$$S_{\mathcal{APT}}(\omega) = \frac{1}{m'_{22}} \begin{pmatrix} m'_{12} & 1 \\ 1 & -m'_{21} \end{pmatrix}, \quad (13)$$

from which we immediately find (3) using (11).

The phase transition of the S-matrix can be inferred from the relations (3), which suggest the parametrization of the S-matrix by three independent *real* quantities: t , $a \equiv \text{Re}[r_L]$, and $b \equiv \text{Im}[r_L]$, i.e.

$$S = \begin{pmatrix} a + ib & t \\ t & a - ib \end{pmatrix}, \quad (14)$$

which is pseudo-Hermitian [23], i.e. $S^\dagger = \eta S \eta^{-1}$ with $\eta = \begin{pmatrix} 0 & 1 \\ 1 & 0 \end{pmatrix}$. The eigenvalues of the S-matrix are given by

$$s_{\pm} = a \pm \sqrt{t^2 - b^2}, \quad (15)$$

which have two phases and the phase transitions occur at $t = \pm b$. The scattering eigenstates $\psi_{\pm}(\omega) = \begin{pmatrix} B_{\pm} \\ C_{\pm} \end{pmatrix}$ display a transition simultaneously:

$$p_{\pm} \equiv \frac{B_{\pm}}{C_{\pm}} = \frac{1}{t} [ib \pm \sqrt{t^2 - b^2}]. \quad (16)$$

In one phase ($|t| > |b|$) the intensities of the two incident beams in a scattering eigenstate are the same, i.e. $|p_{\pm}| = 1$ (see Fig. 2). Thus we refer to this phase as the symmetric scattering phase and the other as the symmetry-broken phase ($|t| < |b|$). In the symmetric phase s_{\pm} are real, meaning that the symmetric inputs are either amplified or damped equally with no phase added during the scattering process. In the symmetry-broken phase the two scattering eigenstates have the same scattering strength $|s|$ ($s_+ = s_-$) but with $|p_+| = |p_-|^{-1}$.

Tuning to the phase transition points requires adjusting either the gain/loss parameter of the system, the frequency of incident beam, or scaling the system size. Given that it is challenging to maintain \mathcal{APT} (or \mathcal{PT}) symmetry in the first two approaches due to material dispersion, the third approach is probably most practical, i.e. by fabricating multiple scaled heterostructures and fixing the frequency of incident beams at a value that achieves the \mathcal{APT} symmetry.

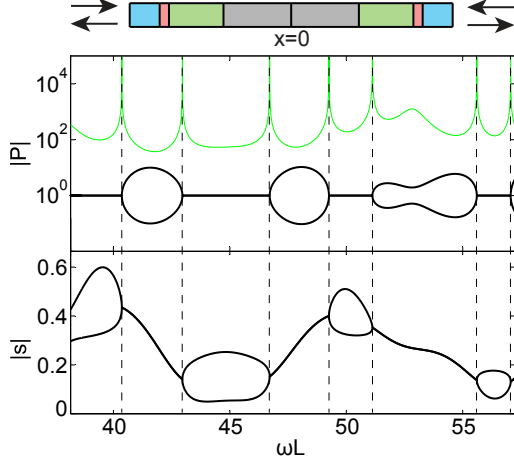


FIG. 2. (Color online) Phase transition of the S-matrix in an \mathcal{APT} heterostructure. Top: An 8-layers example with $\text{Re}[n_i] = 1.3, -2, -1.7, -3$, $\text{Im}[n(x)] = 0.04$ (loss), and width $\Delta_i = 1.2, 0.996, 0.165, 0.531 \mu\text{m}$ ($i = 1, 2, 3, 4$) for $x > 0$. Thick solid black lines in the middle and bottom panels show the transitions of the asymmetry factor $|p|$ and the scattering strength $|s|$. Thin solid green line in the middle panel indicates $|t|^2 - \text{Im}[r_L]^2$, which approaches infinite at the phase transition points marked by the dashed vertical line.

The phase transition discussed above is a general properties of all 1D \mathcal{APT} systems, independent of whether the system has net gain or loss. By flipping the sign of $\text{Im}[n(x)]$, i.e. changing local gain into loss and vice versa, the system merely undergoes a time reversal and the phase transitions happen at exactly the same locations.

There is only one exception which occurs when the local gain/loss is zero [24], i.e. $\text{Im}[n(x)] = 0$. In this case an \mathcal{APT} heterostructure is always in the symmetric phase. More strikingly, the relations (3) now take a special form:

$$t = 1, \quad r_L = r_R = 0, \quad (17)$$

i.e. an \mathcal{APT} system becomes invisible, and it is independent of the complexity and size of the heterostructure and at what frequency the \mathcal{APT} symmetry occurs. This phenomenon is robust upon a slight breakdown of the \mathcal{APT} -symmetry or in the presence of a small $\text{Im}[n(x)] \neq 0$ (see Fig. 3(a)). In addition, the invisibility is independent of whether the \mathcal{APT} structure is standalone or integrated in a photonic environment, as long as the nearest elements have the same refractive index (see Fig. 3(b)). If the \mathcal{APT} symmetry can be maintained over a finite frequency range, a pulse transmitted within this frequency window will be exactly the same as the initial pulse, with no pulse distortion or shrinking/expansion. This phenomenon is independent of the propagation direction, in contrast to the one-way invisibility found in \mathcal{PT} -symmetric heterostructures [12].

The relations (17) can be treated as a generalization of the phenomenon of vanished reflection that happens at

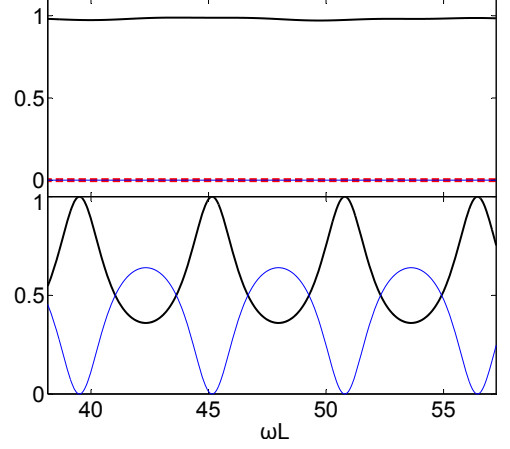


FIG. 3. (Color online) Top: Transmittance and reflectance in the \mathcal{APT} photonic heterostructure shown in Fig. 2 but with $\text{Im}[n(x)] = 10^{-4}$ (loss). Thick black line, thin blue line, and dotted red line indicate $T = |t|^2$, $R = |r_L|^2 \approx |r_R|^2$, and $\text{Arg}[t]$, respectively. They are very close to the values given by (17), i.e. 1, 0, 0, when $\text{Im}[n(x)] = 0$. Bottom: Same as the top panel but $\text{Re}[n_4]$ changes from -3 to 3. The oscillations in R and T have a single period determined by the combined width of the leftmost and rightmost layers, i.e. $\Delta\omega L = \pi L / (2\Delta_4 \text{Re}[n_4]) = 5.64$, as if the central 6-layer \mathcal{APT} structure is absent.

the interface of two impedance matched PIM and NIM materials (see Ref. [14] for example). There is at least one such interface in an \mathcal{APT} system, i.e. at $x = 0$, but multiple reflections occur at other interfaces between two NIMs, two PIMs, and a NIM and a PIM of different $|n|$. One way to prove (17) is from the transfer matrix $M_{\mathcal{APT}}(\omega)$ directly:

$$M_{\mathcal{APT}}(\omega) = D_0^{-1} [\Pi_{i=-N}^N m_i] D_0, \quad i \neq 0. \quad (18)$$

Note that

$$m_{-i}(\omega) m_i(\omega) = 1 \quad (19)$$

when n_i is real. Therefore,

$$M_{\mathcal{APT}}(\omega) = D_0^{-1} [\Pi_{i=-N, \dots, -2, 2, \dots, N} m_i] D_0 = \dots = 1, \quad (20)$$

which implies (17).

Net gain has been demonstrated in NIMs by imbedding an active medium [19], which opens the possibility of achieving lasing in metamaterials. Lasing modes are given by the poles of the S-matrix on the real frequency axis, which in general lead to discrete set of solutions containing the lasing frequency $\omega_L^{(m)}$ and the corresponding threshold $\tau^{(m)} = -\text{Im}[n(x)] > 0$ assuming a spatially uniform gain. Each lasing mode has its distinct intensity profile and roughly speaking the mode order m indicates the number of peaks inside the cavity. To determine $\{\omega_L, \tau\}$ for each mode, one can, for example, solve the two equations given by the real and imaginary part of m'_{22} in 1D heterostructures (see Eq. (13)). However,

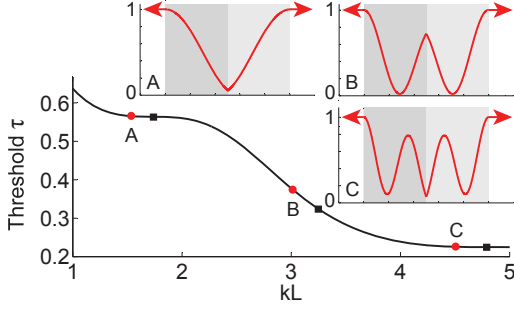


FIG. 4. (Color online) (a) Threshold value $\tau(\omega_L)$ for the continuous lasing spectrum in a 2-layer \mathcal{APT} heterostructure. Each layer is 500nm thick and the refractive indices are $\pm 2 - i\tau(\omega_L)$ at threshold. Squares indicate the discrete lasing solutions $\omega L = 1.735, 3.245, 4.786$ in a uniform PIM cavity of the same length. Inset: Intensity profiles at $\omega L = 1.5, 3, 4.5$ marked by the red dots in the main figure. Shadowed areas indicate the cavity. (b) Number of lasing modes in the region $kL_0 < 30$ versus the width of one layer in (a).

Eq. (11) shows that m'_{22} is always real for an \mathcal{APT} system, which implies that there exist continuous regions of ω_L in which a ω_L -dependent τ can be found. In other words, a lasing mode can appear anywhere in these frequency regions and a mode order m cannot be assigned. A 2-layer \mathcal{APT} structure in the low frequency regime is shown as an example in Fig. 4. We observe a reduced threshold as the lasing frequency increases and more oscillations gradually appear in the intensity profile. If we consider the lasing modes in the corresponding PIM cavity of the same length and $|n|$, we find that its discrete lasing solutions lie exactly on the continuous threshold curve of the \mathcal{APT} structure (see Fig. 4 and Appendix A). This comparison also shows that coherent feedback does occur in a \mathcal{APT} -system based laser, even though the its spectrum is continuous.

Unlike the bidirectional invisibility, the continuous lasing spectrum is singular and breaks down if the \mathcal{APT} -symmetry is broken, which can be utilized as a sensitive measure of the quantities of interest that lead to the latter. Here we consider one scenario where the \mathcal{APT} -symmetry is broken due to a slight length mismatch. Consider a 2-layer cavity of length L similar to that studied in Fig. 4 but with the PIM layer δ longer than the NIM layer. We found that all lasing modes disappear except the ones at $kL \approx m\pi L/(|n|\delta)$ ($m = 1, 2, \dots$), whose thresholds are about the same when the \mathcal{APT} -symmetry is satisfied. Take $L = 250\mu\text{m}$, $\delta = 250\text{nm}$, and $|n| = 2$ for example, the corresponding wavelengths are $\lambda = m^{-1}\mu\text{m}$, which are well separated and easy to achieve single-mode lasing. These modes originate from the resonances of the tiny section of length δ , which acts as an external cavity for frequency selection. In this example, the variation of δ (or L) is enhanced by four times in the wavelength of the fundamental mode ($m = 1$) since $\Delta\lambda = 4\Delta\delta/m$, which can be easily measured. As a comparison, the sensitivity to detect δ is reduced by a factor

of $\delta/L = 10^{-3}$ using a lasing mode of roughly the same wavelength in a uniform PIM cavity of length L , which also has a much denser spectrum to analyze. We note that the laser linewidths are comparable in the two systems, since the thresholds of the corresponding modes are about the same as discussed.

So far we have discussed the \mathcal{APT} symmetry with balanced PIMs and NIMs. One may attempt to realize a “pseudo- \mathcal{APT} ” symmetry using only PIMs (or NIMs), satisfying $n(x) = -n(-x)^*$ but with $\mu(x) = \mu(-x)$. One example in which such symmetry can be realized is wave propagation in 2D paraxial geometry [4, 5], with transverse index variation $n(x) = n_0 + \delta n(x)$ satisfying $|\delta n(x)| \ll n_0$ and $\delta n(x) = -\delta n(-x)^*$. The Helmholtz equation (1) in this case becomes [5]

$$i\frac{\partial\phi}{\partial z} + \left[\frac{\partial^2}{\partial \tilde{x}^2} + \delta n(\tilde{x})k_0 \right] \phi = 0, \quad (21)$$

where $\phi(x, z)$ is the slowly varying part of the electrical field $E(x, z) = \phi(x, z)e^{ik_0 z}$ and $\tilde{x} = \sqrt{2n_0 k_0}x$ is the scaled coordinate in the transverse direction. The transverse optical potential now is proportional to $\delta n(\tilde{x})$ instead of index squared in the original Helmholtz equation (1), and the intriguing phenomena discussed above disappear. The only exception happens when the system becomes equivalent to a conventional \mathcal{PT} -symmetric structure. The latter occurs, for example, if $\delta n(\tilde{x}) = A \sin \tilde{x} + iB \cos \tilde{x}$ ($A, B \in \mathbb{R}$); shifting \tilde{x} by $\pi/2$ transforms $\delta n(\tilde{x})$ to $A \cos \tilde{x} - iB \sin \tilde{x}$, satisfying $n(\tilde{x}) = n(-\tilde{x})^*$.

In summary, we propose a new class of synthetic materials which are antisymmetric under a combined parity-time operation, i.e. $n(\mathbf{x}) = -n(-\mathbf{x})^*$. \mathcal{APT} systems demonstrate interesting features such as bidirectional invisibility, spontaneous phase transition of the S-matrix, and a continuous lasing spectrum. Properties of \mathcal{APT} systems in higher dimensions are under investigation and will be reported elsewhere.

We acknowledge Douglas Stone and Kostas Makris for helpful discussions. This research was supported by MIRTHER NSF EEC-0540832.

Appendix A: Threshold correspondence in a simple \mathcal{APT} heterostructure and a PIM cavity

The threshold $\tau(\omega_L)$ of the continuous lasing spectrum in a simple 2-layer cavity discussed in the main text is given by the solution of the *real* equation

$$|\cos \alpha|^2 + \frac{n_r^2 - \tau^2}{n_r^2 + \tau^2} |\sin \alpha|^2 = -\text{Im} \left[\left(n_r - i\tau + \frac{1}{n_r - i\tau} \right) \sin \alpha (\cos \alpha)^* \right], \quad (\text{A1})$$

in which n_r is the real part of the refractive index in the PIM, $\alpha \equiv (n_r - i\tau)\omega_L L/2$, and L is the cavity length. In comparison, the threshold and the discrete lasing frequency in a uniform PIM cavity of the same length

are simultaneously determined by the following *complex* equation

$$\cos(2\alpha) = i \left[\left(n_r - i\tau + \frac{1}{n_r - i\tau} \right) \sin \alpha \cos \alpha \right]. \quad (\text{A2})$$

It implies that

$$\tan \alpha = -i(n_r - i\tau), -\frac{i}{n_r - i\tau}, \quad (\text{A3})$$

or

$$\text{Re} \left[\frac{\tan \alpha}{(\tan \alpha)^*} \right] = \frac{n_r^2 - \tau^2}{n_r^2 + \tau^2}. \quad (\text{A4})$$

By taking the real part of both sides of (A2) after multiplying them by $(\cos \alpha)^* / \cos \alpha$, we find

$$\begin{aligned} & |\cos \alpha|^2 + \text{Re} \left[\frac{\tan \alpha}{(\tan \alpha)^*} \right] |\sin \alpha|^2 \\ &= -\text{Im} \left[\left(n_r - i\tau + \frac{1}{n_r - i\tau} \right) \sin \alpha (\cos \alpha)^* \right], \end{aligned} \quad (\text{A5})$$

from which we recover (A1) using (A4).

-
- [1] C. M. Bender and S. Boettcher, Phys. Rev. Lett. **80**, 5243 (1998).
 - [2] C. M. Bender, S. Boettcher, and P. N. Meisinger, J. Math. Phys. **40**, 2201 (1999).
 - [3] C. M. Bender, D. C. Brody, and H. F. Jones, Phys. Rev. Lett. **89**, 270401 (2002).
 - [4] R. El-Ganainy, K. G. Makris, D. N. Christodoulides, and Z. H. Musslimani, Opt. Lett. **32**, 2632–2634 (2007).
 - [5] K. G. Makris, R. El-Ganainy, D. N. Christodoulides, and Z. H. Musslimani, Phys. Rev. Lett. **100**, 103904 (2008).
 - [6] C. E. Rüter, K. G. Makris, R. El-Ganainy, D. N. Christodoulides, M. Segev, and D. Kip, Nat. Phys. **6**, 192 (2010).
 - [7] M. C. Zheng, D. N. Christodoulides, R. Fleischmann, and T. Kottos, Phys. Rev. A **82**, 010103(R) (2010).
 - [8] Y. D. Chong, Li Ge, H. Cao, and A. D. Stone, Phys. Rev. Lett. **105**, 053901 (2010).
 - [9] W. Wan, Y. D. Chong, L. Ge, H. Noh, A. D. Stone and H. Cao, Science **331**, 889 (2011).
 - [10] S. Longhi, Phys. Rev. A **82**, 031801 (R) (2010).
 - [11] Y. D. Chong, Li Ge, and A. D. Stone, Phys. Rev. Lett., **106**, 093902 (2011).
 - [12] Z. Lin, H. Ramezani, T. Eichelkraut, T. Kottos, H. Cao, and D. N. Christodoulides, Phys. Rev. Lett. **106**, 213901 (2011).
 - [13] L. Ge, Y. D. Chong, and A. D. Stone, Phys. Rev. A **85**, 023802 (2012).
 - [14] J. B. Pendry, Phys. Rev. Lett. **85**, 3966–3969 (2000).
 - [15] V. Shalaev *et al.*, Opt. Lett. **30**, 3356 (2005).
 - [16] G. Dolling *et al.*, Opt. Lett. **32**, 53 (2007).
 - [17] J. Valentine *et al.*, Nature **455**, 376 (2008).
 - [18] H. N. S. Krishnamoorthy, Z. Jacob, E. Narimanov, I. Kretzschmar, and V. M. Menon, Science **13**, 205–209 (2012).
 - [19] S. Xiao *et al.*, Nature **466**, 735738 (2010).
 - [20] P. Schmidt, I. Grigorenko, and A. F. J. Levi, J. Opt. Soc. Am. B **24**, 2791 (2007).
 - [21] J. Wiersig *et al.*, Phys. Rev. A **81**, 023809 (2010).
 - [22] A. Yeh, *Optical waves in layered media* (Wiley, New York, 1988).
 - [23] A Mostafazadeh, J. Math. Phys. **43**, 205 (2002).
 - [24] An active medium is required in the NIM layers to compensate the intrinsic loss to reach this condition.